IEEE *Access*
Multidisciplinary ⋮ Rapid Review ⋮ Open Access Journal

A Profit-Maximizing Security-Constrained IV-AC Optimal Power Flow Model & Global Solution

AMRO M. FARID [iD], **(Senior Member, IEEE)**
Thayer School of Engineering, Dartmouth College, Hanover, NH 03755, USA
MIT Department of Mechanical Engineering, Cambridge, MA 02139, USA

e-mail: amfarid@dartmouth.edu; amfarid@mit.edu

ABSTRACT Since its first formulation in 1962, the Alternating Current Optimal Power Flow (ACOPF) problem has been one of the most important optimization problems in electric power systems. Its most common interpretation is a minimization of generation costs subject to network flows, generator capacity constraints, line capacity constraints, and bus voltage constraints. The main theoretical barrier to its solution is that the ACOPF is a non-convex optimization problem that consequently falls into the as-yet-unsolved space of NP-hard problems. To overcome this challenge, the literature has offered numerous relaxations and approximations of the ACOPF that result in computationally *suboptimal* solutions with potentially *degraded reliability*. While the impact on reliability can be addressed with active control algorithms, energy regulators have estimated that the sub-optimality costs the United States ~$6-19B per year. Furthermore, and beyond its many applications to electric power system markets and operation, the sustainable energy transition necessitates renewed attention towards the ACOPF. This paper contributes a profit-maximizing security-constrained current-voltage AC optimal power flow (IV-ACOPF) model and *globally optimal* solution algorithm. More specifically, it features a convex separable objective function that reflects a two-sided electricity market. The constraints are also separable with the exception of a set of linear network flow constraints. Collectively, the constraints enforce generator capacities, thermal line flow limits, voltage magnitudes, power factor limits, and voltage stability. The optimization program is solved using a Newton-Raphson algorithm and numerically demonstrated on the data from a transient stability test case. The theoretical and numerical results confirm the globally optimal solution.

INDEX TERMS Electric power systems engineering, optimization, optimal power flow, ACOPF, DCOPF, electricity markets.

I. INTRODUCTION

Since its first formulation in 1962 [1], the Alternating Current Optimal Power Flow (ACOPF) problem has been one of the most important optimization problems in electric power systems. Its most common interpretation is a minimization of generation costs subject to network flows, generator capacity constraints, line capacity constraints, and bus voltage constraints [2], [3]. Although a globally optimal solution to the ACOPF itself remains elusive, its most common approximation, the DCOPF (Direct Current Optimal Power Flow), has been at the heart of many wholesale deregulated "real-time" energy markets found at many North American Independent System Operators (ISOs) [4]–[6]. Furthermore, the DCOPF often serves as the "sub-problem" in mixed-integer, security-

The associate editor coordinating the review of this manuscript and approving it for publication was Ali Raza [iD].

constrained, unit commitment optimization models [7]–[10] and generation and transmission planning models [11]–[14]. These, in turn, serve as the basis of wholesale "day-ahead" energy markets in the same ISOs. Beyond these "economic-control" applications, the ACOPF has also served as a reliability tool for grid operators. The generation cost objective function can also be replaced with a minimization of electric power losses or load-shedding amongst other operational objectives depending on grid conditions [2], [3].

Consequently, these many applications have motivated extensive attention towards the ACOPF. The main theoretical barrier is that the ACOPF is a non-convex optimization problem and thus falls into the as-yet-unsolved space of NP-hard problems [3]. To overcome the lack of convexity, the literature has offered numerous relaxations and approximations of the non-convex constraints including: the copper plate relaxation, the network flow relaxation,

TDC-0008268

Case 1:23-cv-00426-SM   Document 38-8   Filed 05/01/25   Page 2 of 9
A. M. Farid: Profit-Maximizing Security-Constrained IV-ACOPF Model & Global Solution

IEEE Access

the Second Ordered Cone Programming (SOCP) relaxation, the Quadratic Convex (QC) relaxation, the Semi-Definite Programming relaxation (SDP), and the well-known DCOPF approximation [15]. These approaches result in computationally feasible, polynomial-time algorithms at the expense of potentially degraded reliability. In addition to the above, the literature has also offered numerous non-deterministic optimization methods including: Evolutionary Algorithms (EAs) [16]–[20], Particle Swarm Optimization (PSO) [21]–[27], Simulated Annealing (SA) [28]–[30], Artificial Neural Networks (ANN) [31]–[34], and Chaos Optimization Algorithms (COA) [35]. Despite these advances, the classification of the ACOPF in the NP-hard space has meant that a globally optimal solution remains elusive to either the detriment of system reliability or electricity costs. One author at FERC (Federal Energy Regulatory Commission) estimates that more efficient market dispatch can save the United States ~$6-19B per year [3].

Although the ACOPF problem already has an extensive history, the sustainable energy transition necessitates renewed attention. 1) First, in order to support the integration of distributed generation [36]–[39] and energy storage [40], electric power system markets are expanding beyond their traditional implementation as wholesale markets in the transmission system to retail markets in the distribution system [41]–[45] and microgrids [46]–[50]. This constitutes a dramatic proliferation of the optimal power flow problem from the nine North American independent system operators to potentially thousands of electric distribution system utilities [51]. 2) Furthermore, the radial and large-scale nature of distribution systems necessitates scalable ACOPF algorithms [36], [52]–[54]. 3) Distribution systems must also feature a prominent role for line losses, nodal voltages, and reactive power flows which disqualifies many of the typical OPF approximations [52]. 4) Fourth, the integration of variable renewable energy resources further necessitates the participation of demand-side resources in two-sided markets [36], [53], [54]. 5) Finally, as the electric power grid activates these demand–side resources, it also integrates itself with the operation of other infrastructures including water [55]–[58], transportation [59], industrial production [60], natural gas [61]–[64] and heat [65]–[68]. The non-linearity and non-convexity of the electric power network flow equations – as they are commonly stated – impedes the effective coupling of multiple infrastructure sectors. Collectively, these reasons indicate that the ACOPF problem needs an alternative formulation and not just a new solution algorithm. Furthermore, it is of immediate importance to many grid stakeholders including transmission system operators, distribution system operators, and electric utilities.

A. ORIGINAL CONTRIBUTION

The original contribution of this paper is a profit-maximizing security-constrained current-voltage AC optimal power flow (IV-ACOPF) model and globally optimal algorithm. The main novelties are as follows. 1) This ACOPF formulation has as decision variables, the real and imaginary components of the generator currents, the real and imaginary components of the line currents, and the real and imaginary components of the generator and bus voltages. Unlike other IV-ACOPF formulations, active and reactive power variables are not included to avoid non-convex feasible regions. The reliance on IV variables eliminates the non-convexities of the network flow constraints. 2) Rather than using the "power-flow analysis" model, a steady-state current-injection model of the physical power grid is used. As a result, generator terminal voltages are connected to exactly one other bus through a lead line. 3) A profit maximization objective function is introduced so as to create an explicit two-sided (rather than one-sided) energy market. 4) Box constraints on generator current capacities are derived from the capability curves of synchronous generators. 5) Unlike other ACOPF formulations where they are often neglected, voltage stability constraints are introduced for further reliability. 6) Finally, a power factor constraint is included as a reliability requirement enforced by many grid codes [69], [70]. This new reformulation of the ACOPF is solved via a Newton-Raphson algorithm and proven to converge to the globally optimal solution in polynomial time. The numerical results confirm a globally optimal solution for feasible loading conditions and returns an infeasible result otherwise. The paper proves that the provided IV-ACOPF formulation is a generalization of the familiar ACOPF in $PQV\theta$ variables.

B. PAPER OUTLINE

The remainder of this work is structured as follows: In Section II, a typical ACOPF formulation is introduced and some of the recent solution algorithms are presented. Section III derives the new formulation of the IV-ACOPF and proves its classification as a convex optimization program. Section IV presents the Newton-Raphson solution algorithm and proves its convergence to the globally optimal solution. Section V, then, demonstrates the IV-ACOPF formulation and solution on data from a well-known transient stability test case. Section VI discusses the novel features of this IV-ACOPF reformulation and concludes that it is a generalization of the ACOPF in $PQV\theta$ variables. Finally, Section VII concludes the work.

II. BACKGROUND

The first full formulation of the Optimal Power Flow (OPF) problem was presented by Carpentier in 1962 [1]. Since then, faster computational resources, the restructuring of electricity markets, and the proliferation of diverse (physical) energy resources on the grid have resulted in a rich volume of OPF literature spanning six decades. Surveys that look at the evolution and different approaches to solving the problem include [3], [35], [71]–[79]. Most typically, the objective function of the OPF problem is the minimization of generation costs or maximization of power grid profit. However, operators often choose other objectives including the mini-

mization of losses, the minimization of load-shedding, among other possibilities.

Equations 1-7 collectively depict a typical formulation of the ACOPF problem using '$PQV\theta$' decision variables.

$$\min \quad \sum_{g \in \mathcal{G}} \left(\alpha_{Rg} P_g^2 + \beta_{Rg} P_g + \gamma_{Rg} \right) \tag{1}$$

$$- \sum_{d \in \mathcal{D}} \left(\alpha_{Rd} P_d^2 + \beta_{Rd} P_d + \gamma_{Rd} \right)$$

$$s.t. \quad \sum_{g \in \mathcal{G}} A_{gd} P_g - P_d \tag{2}$$

$$= |V_d| \sum_{d' \in \mathcal{D}} |V_{d'}| \left(g_{dd'} \cos(\theta_{dd'}) + b_{dd'} \sin(\theta_{dd'}) \right)$$

$$\forall d \in \mathcal{D}$$

$$\sum_{g \in \mathcal{G}} A_{gd} Q_g - Q_d \tag{3}$$

$$= |V_d| \sum_{d' \in \mathcal{D}} |V_{d'}| \left(g_{dd'} \sin(\theta_{dd'}) - b_{dd'} \cos(\theta_{dd'}) \right)$$

$$\forall d \in \mathcal{D}$$

$$\theta_{v1} = 0 \tag{4}$$

$$P_g^{min} \le P_g \le P_g^{max} \qquad \forall g \in \mathcal{G} \tag{5}$$

$$Q_g^{min} \le Q_g \le Q_g^{max} \qquad \forall g \in \mathcal{G} \tag{6}$$

$$0 \le P_\ell \le P_\ell^{max} \quad \forall \ell \in \mathcal{L} \tag{7}$$

$$|V_d|^{min} \le |V_d| \le |V_d|^{max} \qquad \forall d \in \mathcal{D} \tag{8}$$

To elaborate, this formulation uses the "power flow analysis" model of an electric power system. It includes a set of demand buses $\mathcal{D}$ with its associated vector of voltage phasors $V_D = |V_D| \angle \theta_{VD}$ as decision variables and complex power withdrawals $S_D = P_D + jQ_D$ as imposed exogenous constants. Consequently, this typical formulation assumes *inelastic demand* for electric power. The power system model also includes a set of generators $\mathcal{G}$ with its associated vector of complex power injections $S_G = P_G + jQ_G$ as decision variables. The power system model also includes power lines $\mathcal{L}$. These have their associated vector of complex power flows $S_\mathcal{L} = P_L + jQ_L$ as decision variables. The model relies on the formulation of a bus admittance matrix $Y = G + jB$ such that the subscript notation of the scalars $g_{dd'}$ and $b_{dd'}$ indicate the (d,d') element of the G and B matrices respectively. Similarly, the notation $\theta_{dd'}$ is the voltage phase angle difference between demand buses d and d'. A_{GD} is the generator to demand bus incidence matrix indicating a value of 1 when generator g is connected to bus d. Finally, α_{Rg}, β_{Rg}, and γ_{Rg} are the quadratic, linear, and fixed cost terms of the active power injections by each generator $g \in \mathcal{G}$ and α_{Rd}, β_{Rd}, and γ_{Rd} are the quadratic, linear, and fixed terms of the active power withdrawals at each demand bus $d \in \mathcal{D}$.

As a whole, this formulation of the ACOPF maximizes profit subject to physical reliability constraints. Equation 1 is the (negative) profit objective function (to be minimized) that is composed of a convex quadratic cost function of the active power generated and a convex quadratic revenue function

of the active power consumed. Note that because the vector of active power demands P_D is an *exogeneous constant*, the revenue terms in this *two-sided market formulation* are very commonly dropped to produce an *equivalent one-sided market formulation* in which the objective function is written as a simple minimization of generation costs:

$$\min \sum_{g \in \mathcal{G}} \alpha_{Rg} P_g^2 + \beta_{Rg} P_g + \gamma_{Rg} \tag{9}$$

Equation 2 is the network flow constraint for active power, Equation 3 is the network flow constraint for reactive power, Equation 4 indicates the reference angle of the network, Equation 5 is the active power capacity constraint, Equation 6 is the reactive power capacity constraint, Equation 8 is the voltage magnitude constraint at a bus, and Equation 7 is the line flow limit constraint. Also note that Equations 2 and 3 collectively make the ACOPF problem non-linear and non-convex. In order to overcome the problems caused by the non-linearity and non-convexity of these constraints, an extensive literature has emerged that proposes numerous relaxations, approximations, and solution algorithms.

Perhaps the most commonly deployed approximation, especially in electric energy markets, is the so-called "DCOPF" problem [3]. It is obtained by setting all voltage magnitudes to unity, eliminating lines losses (i.e. G = 0), and linearizing the power flow equations via a small-angle approximation [80]. Despite its broad adoption, the DCOPF approximation cannot be used universally; including in distribution systems where line losses are non-negligible [52]. Furthermore, a DCOPF solution may not satisfy the original nonlinear power flow equations. Under such circumstances, an operator might tweak the DCOPF solution through a subsequent solution of the power flow analysis equations. The DCOPF can also over-constrain the solution space; potentially generating an infeasible solution even when the ACOPF remains feasible. Finally, there is no guarantee that the obtained DCOPF solution is either locally or globally optimal and estimation of the distance from global optimality remains a topic of research [81].

Consequently, much of the recent ACOPF literature has sought to use reformulations that involve Convex Relaxations (CR). In such works, non-convex constraints are loosened to form a larger, but more importantly, convex feasible region. The main advantage of such an approach is that if the new CR algorithm returns an optimal solution within the original non-convex region, then it has also solved the original (non-convex) problem as well. Furthermore, if the new CR algorithm returns an infeasible solution, then the original (non-convex) problem was as well. Several CRs have appeared in the recent ACOPF literature. One of the most promising relaxations to the ACOPF problem, the Second Order Cone Programming (SOCP) was proposed for radial networks by Jabr in 2006 [82]. Since then, the semi-definite programming (SDP) relaxation has garnered a lot of attention for its robustness and performance in the literature

[83]–[85]. In particular, Lavaie and Low have shown topological conditions where the SDP relaxation demonstrates a zero duality gap and, therefore, returns a globally optimal solution [86]. Finally, the Quadratic Convex (QC) relaxation has been shown to be promising, producing results that are also robust and reliable [87]. It has also been shown that certain types of network topologies can guarantee a globally optimal solution [88], [89]. For radial networks, some of the aforementioned relaxations have proved to be equivalent, with a bijective map between their feasible set [90].

Finally, a relatively small portion of the ACOPF literature abandons the active power (P), reactive power (Q), voltage magnitude ($|V|$), and voltage phase angle (θ) decision variables in favor of novel combinations of not just P and Q but also the voltage (V) and current phasors ($\mathcal{I}$) in rectangular coordinates. A rectangular IV-PQ formulation has been proposed and has demonstrated good computational performance despite a lack of convexity [75], [91], [92]. A power-current hybrid formulation has also been proposed with similar effect [93]. The premise of these works is the assertion that if the non-convexity in the network wide flow constraint can be isolated to the buses and made separable, the formulation becomes more amenable to a relaxation [75], [91]. The following section proceeds within this general category of IV-ACOPF formulations with several novel additions.

III. IV-ACOPF FORMULATION

This section derives an IV-ACOPF formulation in rectangular coordinates using a current-injection model [94] equivalent to the one use in transient stability analysis studies after steady-state conditions have been achieved. As is elaborated in Section VI, this steady-state current injection model provides many advantages; most notably the ability to separate all power system nodes into two distinct groups; generator terminals and demand-buses. In addition to the constraints found in the traditional formulation of the optimal power flow problem, three additional physical phenomena are included in this formulation. First, a current injection model rather than power flow analysis model is used. Therefore, each generator receives its associated lead line in the network flow [94], [95]. Second, voltage stability imposes a constraint on the difference in voltage phase angle between two buses [94], [95]. Some $PQV\theta$ formulations have introduced voltage stability constraints [96]–[99], but an extensive search has yet to reveal their introduction into an IV-ACOPF. Lastly, the net power injection into a given bus is placed within minimum and maximum power factor limits to reflect IEEE operating standards [95].

The elaboration of the IV-ACOPF formulation proceeds as follows. Sec. III-A contrasts the current injection model to the power flow analysis model. Sec. III-B then derives the associated network flow equations from first engineering principles. Next, Sec. III-C derives the objective function from first economic principles. The section then follows the ACOPF formulation described in Section II with

Sec. III-D, III-E, III-F and III-G describing the reference voltage, generator capacity, thermal line flow, voltage magnitude constraints respectively. The power factor and voltage stability constraints are then added as new constraints in Sections III-H and III-I respectively. Finally, in order to create a convex feasible region, a high quality relaxation of the voltage magnitude lower bound is introduced in Sec. III-J. Section IV later proves that the introduction of such a relaxation does not impede a solution to a global optimum.

A. THE STEADY-STATE CURRENT INJECTION MODEL

The current injection model is a well established power systems engineering model that is used to study the "transient (angle) stability" of a power system in response to various disruptions [94], [95]. The power flow analysis model used in the traditional ($PQV\theta$) ACOPF problem above corresponds with the green buses and blue lines in Fig. 1. Generators and loads appear as power injections directly into or out of these buses. The current injection model, instead, treats each generator as a voltage source attached to a lead line. For transient stability analyses, usually in the 0.1-10Hz timescale, each of these generators is given a differential equation called a "swing equation". Then the system-wide stability is assessed either by numerical simulation in response to a perturbation or directly by analytical methods. As the optimal power flow problem is typically run every five minutes, one can reasonably assume that swing equation dynamics have reached steady state and can be subsequently neglected for the remainder of the paper.
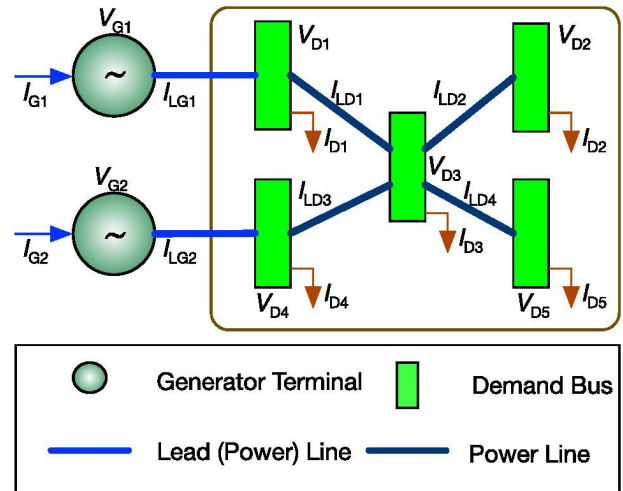

FIGURE 1. The Power Flow Analysis vs the Steady State Current Injection Model. The power flow analysis model includes the green buses, their associated power demands, and the blue power lines. Generators are modeled as power injections directly into some of the buses. The current injection model replaces these power injections with a lead line attached to a generator represented as a voltage source with its associated current injection [94], [95].

As shown in Figure 1, this steady-state current injection model has a set of demand buses $\mathcal{D}$ with its associated vector of voltages $V_D = V_{DR} + jV_{DI}$ and current withdrawals $\mathcal{I}_D = \mathcal{I}_{DR} + j\mathcal{I}_{DI}$ which are taken as exogenous data inputs.

TDC-0008271

It also has a set of generators $\mathcal{G}$ with its associated vector of voltages $V_G = V_{GR} + jV_{GI}$ and current injections $\mathcal{I}_G = \mathcal{I}_{GR} + j\mathcal{I}_{GI}$. The power lines $\mathcal{L} = \mathcal{L}_G \cup \mathcal{L}_D$ are partitioned into lead lines $\mathcal{L}_G$ and the power lines $\mathcal{L}_D$ of the original power flow analysis network. These have their associated vector of currents $\mathcal{I}_\mathcal{L} = \mathcal{I}_{\mathcal{L}R} + j\mathcal{I}_{\mathcal{L}I} = [\mathcal{I}_{\mathcal{L}G}; \mathcal{I}_{\mathcal{L}D}]$. The constants $N_\mathcal{G}$, $N_\mathcal{D}$ and $N_\mathcal{L} = N_{\mathcal{L}G} + N_{\mathcal{L}D}$ are also introduced to reflect the number of generators, demand buses, and power lines. The remainder of this section formulates the IV-ACOPF on the basis of this current injection model under steady state conditions. Equations 1-7 are discussed in sequence. As the discussion of the objective function depends on the network flow constraints, the latter are derived first.

B. NETWORK FLOW CONSTRAINTS

Because the network flow equations in Equations 2 and 3 apply to the power flow analysis model and are expressed in PQ variables, they are not a suitable starting point for this derivation. Instead, the network flow equations are re-derived from the first principles of Kirchoff's Current Law and Ohm's law. For the current injection model shown in Fig. 1, Kirchoff's Current Law in rectangular coordinates gives:

$$\begin{bmatrix} \mathcal{I}_{GR} \\ -\mathcal{I}_{DR} \end{bmatrix} = \begin{bmatrix} A_G^T \\ A_D^T \end{bmatrix} \mathcal{I}_{LR} \quad (10)$$

$$\begin{bmatrix} \mathcal{I}_{GI} \\ -\mathcal{I}_{DI} \end{bmatrix} = \begin{bmatrix} A_G^T \\ A_D^T \end{bmatrix} \mathcal{I}_{LI} \quad (11)$$

where $\mathcal{I}_G$ and $\mathcal{I}_D$ have opposite sign convention according to Fig. 1, and where A_G is the line to generator incidence matrix,

$$A_G(l, g) = \begin{cases} 1 & \text{if line } l \text{ originates at generator } g \\ -1 & \text{if line } l \text{ terminates at generator } g \\ 0 & \text{otherwise} \end{cases} \quad (12)$$

and where A_D is the line to bus incidence matrix.

$$A_D(l, d) = \begin{cases} 1 & \text{if line } l \text{ originates at demand bus } d \\ -1 & \text{if line } l \text{ terminates at demand bus } d \\ 0 & \text{otherwise} \end{cases} \quad (13)$$

So as to distinguish between lead lines and power lines shown in Figure 1, it is also useful to partition these incidence matrices: $A_G = [A_{GG}; 0]$ and $A_D = [A_{DG}; A_{DD}]$ and recognize that $A_{DG} = -A_{GD}$ (as defined previously). Then, Ohm's Law in complex matrix form gives:

$$\mathcal{I}_L = Y_L(A_G V_G + A_D V_D) \quad (14)$$

$$\mathcal{I}_L = Y_L[A_G \ A_D] \begin{bmatrix} V_G \\ V_D \end{bmatrix} \quad (15)$$

where $Y_L = G_L + jB_L$ is constructed from the vector of admittances of the lead lines $\mathcal{Y}_G$ and the vector of admittances

of the power lines $\mathcal{Y}_D$. $Y_L = diag(\mathcal{Y}_L) = diag([\mathcal{Y}_{LG}; \mathcal{Y}_{LD}])$. Switching to rectangular components gives:

$$\mathcal{I}_{LR} = G_L[A_G \ A_D] \begin{bmatrix} V_{GR} \\ V_{DR} \end{bmatrix} - B_L[A_G \ A_D] \begin{bmatrix} V_{GI} \\ V_{DI} \end{bmatrix} \quad (16)$$

$$\mathcal{I}_{LI} = B_L[A_G \ A_D] \begin{bmatrix} V_{GR} \\ V_{DR} \end{bmatrix} + G_L[A_G \ A_D] \begin{bmatrix} V_{GI} \\ V_{DI} \end{bmatrix} \quad (17)$$

which simplifies straightforwardly by evaluating the matrix products:

$$\begin{bmatrix} A_G^T \\ A_D^T \end{bmatrix} \mathcal{I}_{LR} = G \begin{bmatrix} V_{GR} \\ V_{DR} \end{bmatrix} - B \begin{bmatrix} V_{GI} \\ V_{DI} \end{bmatrix} \quad (18)$$

$$\begin{bmatrix} A_G^T \\ A_D^T \end{bmatrix} \mathcal{I}_{LI} = B \begin{bmatrix} V_{GR} \\ V_{DR} \end{bmatrix} + G \begin{bmatrix} V_{GI} \\ V_{DI} \end{bmatrix} \quad (19)$$

where G and B are the nodal conductance and susceptance matrices respectively.

$$G = [A_G \ A_D]^T G_L [A_G \ A_D] \quad (20)$$

$$B = [A_G \ A_D]^T B_L [A_G \ A_D] \quad (21)$$

Equations 10, 11, 18 and 19 constitute a steady-state current-injection model and are incorporated into the new IV-ACOPF formulation.

C. OBJECTIVE FUNCTION

Returning back to the objective function of the ACOPF, the translation of the quadratic function in Equation 1 to voltage and current variables requires especially careful attention. Consider a naive change of variable of the active power generated P_g:

$$\begin{aligned} P_g &= \Re\{V_g \mathcal{I}_g^*\} \\ &= \Re\{(V_{Rg} + jV_{Ig})(\mathcal{I}_{Rg} + j\mathcal{I}_{Rg})^*\} \\ &= \Re\{(V_{Rg} + jV_{Ig})(\mathcal{I}_{Rg} - j\mathcal{I}_{Ig})\} \\ P_g &= V_{Rg}\mathcal{I}_{Rg} + V_{Ig}\mathcal{I}_{Ig} \end{aligned} \quad (22)$$

The Hessian of the function in Eq. 22 has eigenvalues $\lambda_e = \{-1, -1, 1, 1\}$ and therefore has indefinite convexity. A similar conclusion is straightforwardly made for a reactive power function of voltage and current. Furthermore, convex functions that are composed of functions of indefinite convexity also have indefinite convexity [100], [101]. This fact serves as a strong caution against any ACOPF reformulation that combines PQ variables with IV variables. Instead, this work develops a formulation on *exclusively* IV variables as shown in the remainder of this work.

The derivation of the objective function $\mathcal{J}$ begins with the well-held economic principle that (in the absence of other constraints) market equilibrium is achieved when the sum of all of Marginal Revenues (MR) and Marginal Costs (MC) equals zero.

$$\nabla J = \sum_{g \in \mathcal{G}} \text{MC}_g - \sum_d \text{MR}_d \quad (23)$$

The earliest works in power system economics; including the first formulations of the economic dispatch, DCOPF, and ACOPF assumed that demand was inflexible and constant in a single time step [102]. Therefore, revenue/utility terms from the demand-side were assumed as constants and were abstracted away in favor of one-sided cost-minimization markets. While this work retains the inflexible and constant demand assumption, the revenue terms are explicitly re-introduced so as to create an explicitly two-sided market with inelastic demand.

Next, each generator is given a linear marginal cost curve and each demand-bus is given a linear marginal revenue curve.

$$\nabla J = \begin{bmatrix} \partial J/\partial P \\ \partial J/\partial Q \end{bmatrix} = \sum_{g \in \mathcal{G}} (\alpha_g \cdot S_g + \beta_g) - \sum_{d \in \mathcal{D}} (\alpha_d \cdot S_d + \beta_d) \tag{24}$$

where $(\cdot)$ is the element-wise Hadamard product [103] and where $\alpha_g = [\alpha_{Rg}; \alpha_{Ig}]$, $\alpha_d = [\alpha_{Rd}; \alpha_{Id}]$, $\beta_g = [\beta_{Rg}; \beta_{Ig}]$, $\beta_d = [\beta_{Rd}; \beta_{Id}]$ are real two-dimensional vectors. Unlike the objective function shown in Eq. 1, this work assumes, for generality, that both active and reactive power generation can incur cost and that active and reactive power consumption can generate revenue. In other words, this IV-ACOPF treats both active and reactive power as monetized and exchanged products. Furthermore, this work retains the common assumption of increasing marginal costs and therefore assumes that both components of α_g are positive. Similarly, this work retains the common assumption of decreasing marginal revenues and therefore assumes that both the components of α_d are negative. Nevertheless, taking the gradient of Eq. 1 immediately results in Eq. 24 with $\alpha_{Ig} = \alpha_{Id} = \beta_{Ig} = \beta_{Id} = 0 \quad \forall g \in \mathcal{G}, d \in \mathcal{D}$.

Several algebraic manipulations are now required in order to convert the non-convex Eq. 24 into an equivalent equation written in IV variables that is convex. Substituting the complex power definition $S = V \star \mathcal{I}^*$ yields:

$$\nabla J = \sum_{g \in \mathcal{G}} (\alpha_g \cdot V_g \star \mathcal{I}_g^* + \beta_g) - \sum_{d \in \mathcal{D}} (\alpha_d \cdot V_d \star \mathcal{I}_d^* + \beta_d) \tag{25}$$

Here the $\star$ notation is introduced to emphasize the multiplication of complex numbers so as to distinguish between matrix multiplication and the element-wise Hadamard product. $[a_R; ja_I] \star [b_R; jb_I] = [a_R b_R + a_I b_I; a_R b_I + a_I b_R]$. In scalar form, Kirchhoff's current balance at each demand-bus d follows from Eq. 10 and 11:

$$-\mathcal{I}_d = \sum_{l \in \mathcal{L}} A_D(l, d) \mathcal{I}_l \tag{26}$$

$$-\mathcal{I}_d = \sum_{l_g \in \mathcal{L}} A_{DG}(l_g, d) \mathcal{I}_{l_g} + \sum_{l_d \in \mathcal{L}} A_{DD}(l_d, d) \mathcal{I}_{l_d} \tag{27}$$

Returning to the linear revenue term $(\alpha_d \cdot V_d \mathcal{I}_d^*)$ in Eq. 25, it is then expressed as a linear combination of revenue components originating from each connected line and lead line. More specifically, complex power coming over a lead line l_g

will have an associated retail rate of $\rho_d + \alpha_g$ while a regular power line will have an associated retail rate of ρ_d.

$$\alpha_d \cdot V_d \mathcal{I}_d^* = -(\rho_d + \alpha_g) \cdot V_d \star \sum_{l_g \in \mathcal{L}_G} A_{DG}(l_g, d) \mathcal{I}_{l_g}^*$$

$$- \rho_d \cdot V_d \star \sum_{l_d \in \mathcal{L}_D} A_{DD}(l_d, d) \mathcal{I}_{l_d}^* \tag{28}$$

where both components of the effective retail rate ρ_d are assumed to be negative to maintain the assumption of diminishing marginal revenues. Recognizing that there is only one lead line l_g for each generator g, and substituting in Eq. 28, Eq. 25 then simplifies to:

$$\nabla J = \sum_{g \in \mathcal{G}} \left(\alpha_g \cdot \left(V_g + \sum_{d \in \mathcal{D}} A_{DG}(g, d) V_d \right) \star I_g^* + \beta_g \right)$$

$$- \sum_{d \in \mathcal{D}} \left(\rho_d \cdot V_d \star I_d^* + \beta_d \right) \tag{29}$$

And then applying Ohm's law yields:

$$\nabla J = \sum_{g \in \mathcal{G}} \left(\alpha_g \cdot Z_g \star I_g \star I_g^* + \beta_g \right) - \sum_{d \in \mathcal{D}} \left(\rho_d \cdot V_d \star I_d^* + \beta_d \right) \tag{30}$$

or simply:

$$\nabla J = \sum_{g \in \mathcal{G}} \left(\alpha_g \cdot S_{\mathcal{L}g} + \beta_g \right) - \sum_{d \in \mathcal{D}} (\rho_d \cdot S_d + \beta_d) \tag{31}$$

where $S_{\mathcal{L}g}$ is the complex power lost in the lead line between a generator and a demand-bus. It must not be confused with the complex power S_g injected by generator g. Furthermore, it is worth noting that Eq. 30 is a convex function of I_g and V_d whereas Eq. 24 is not.

The (negative) profit objective function (to be minimized) is then derived as the sum of the integral of each of the components of the gradient.

$$\mathcal{J} = \int \frac{\partial J}{\partial P_{\mathcal{L}G}} dP_{\mathcal{L}G} + \int \frac{\partial J}{\partial Q_{\mathcal{L}G}} dQ_{\mathcal{L}G}$$

$$+ \int \frac{\partial J}{\partial P_D} dP_D + \int \frac{\partial J}{\partial Q_D} dQ_D \tag{32}$$

which evaluates to:

$$\mathcal{J} = \sum_{g \in \mathcal{G}} \left(\alpha_{Zg} (\mathcal{I}_{Rg}^2 + \mathcal{I}_{Ig}^2)^2 + \beta_{Zg} (\mathcal{I}_{Rg}^2 + \mathcal{I}_{Ig}^2) + \gamma_{Rg} + \gamma_{Ig} \right)$$

$$+ \sum_{d \in \mathcal{D}} \left(\bar{\rho}_{Rd} (V_{Rd} I_{Rd} + V_{Id} I_{Id})^2 - \beta_{Rd} (V_{Rd} I_{Rd} + V_{Id} I_{Id}) + \bar{\gamma}_{Rd} \right)$$

$$+ \left(\bar{\rho}_{Id} (-V_{Rd} I_{Id} + V_{Id} I_{Rd})^2 - \beta_{Id} (-V_{Rd} I_{Id} + V_{Id} I_{Rd}) + \bar{\gamma}_{Id} \right) \tag{33}$$

where $\alpha_{Zg} = (\alpha_{Rg} R_g^2 + \alpha_{Ig} X_g^2)/2$, and $\beta_{Zg} = (\beta_{Rg} R_g + \beta_{Ig} X_g)$. Also, the notation $\bar{\rho}_d = -\rho_d/2$, and $\bar{\gamma}_d = -\gamma_d$ is introduced so as to use positive leading coefficients exclusively. The constants vectors γ_g, γ_{Rd}, and γ_{Id} are introduced to account for the generator fixed costs and demand-bus fixed revenues. Notice that Eq. 33 is a *generalization* of Eq. 1 that accounts

for the cost of reactive power generation and that explicitly includes the revenues from active and reactive power consumption at the demand buses.

Consequently, this objective function implies several locational marginal quantities.

$$\partial J/\partial P_g = \alpha_{Rg} R_g^2 (\mathcal{I}_{R_g}^2 + \mathcal{I}_{I_g}^2) + \beta_{Rg} R_g \tag{34}$$

$$\partial J/\partial Q_g = \alpha_{Ig} X_g^2 (\mathcal{I}_{R_g}^2 + \mathcal{I}_{I_g}^2) + \beta_{Ig} X_g \tag{35}$$

$$\partial J/\partial P_d = \bar{\rho}_{Rd} P_d - \beta_{R_d} \tag{36}$$

$$\partial J/\partial Q_d = \bar{\rho}_{Id} Q_d - \beta_{I_d} \tag{37}$$

These marginal revenue and marginal cost terms tie into the extensive literature on locational marginal prices [104]–[107] and facilitate the use of this IV-ACOPF formulation in electricity market designs despite the novel use of IV variables.

In all, the derived objective function is separable with respect to generator lead lines and demand buses. Furthermore, it is quartic in the lead line currents and quadratic in the demand bus voltages. The work assumes exogenously fixed demand-bus current withdrawals $\mathcal{I}_D$. Although this choice of exogenous data is different from the traditional ACOPF, this data is readily available to grid operators. Furthermore, this choice of exogenous data does maintain the demand-bus voltages as decision variables.

D. REFERENCE VOLTAGE CONSTRAINT

The reference voltage constraint in Equation 4 translates straightforwardly into rectangular components.

$$V_{I_{ref}} = 0 \tag{38}$$

E. GENERATOR CAPACITY CONSTRAINTS

The conversion of the generator capacity "box" constraints in Equations 5 and 6 also requires careful attention. Despite their widespread use, it is important to recognize that there is no physics-based phenomenon that results in box constraints on active and reactive power. Instead, Carpentier's original 1962 paper chose to 1.) assume that all power plants use synchronous generators as electrical machines, and 2.) approximate a synchronous generator's capability curve with a PQ box [1]. The first assumption is entirely appropriate to the reality of predominantly thermo-electric generation in 1962, but is not necessarily valid in the present sustainable energy transition. For Carpentier's second choice, Fig. 2b shows the actual, highly-curved, shape of a synchronous generator's capability curve [108] – which is in turn derived from a synchronous generator's equivalent circuit and phasor diagram [108] (in Fig 2a). The active power upper bound originates from the circular constraint caused by the maximum stator current I_a. Meanwhile, the reactive power upper bound originates from the circular constraint caused by the maximum rotor current (which in turn is proportional to the voltage E_a). The active power lower bound is not an electrical phenomena. Instead, it represents the minimum safe operating level for a combustion-driven process (e.g. boiler or gas turbine) [109]. Fourth, the reactive power lower bound
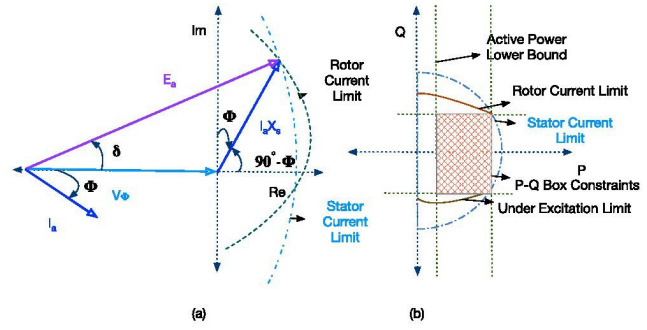

FIGURE 2. (a.) a synchronous generator's phasor diagram and the associated limits on the voltage magnitudes of E_a and $I_a X_S$. (b.) a synchronous generator's actual capability curve and box constraint approximation. [1], [108].

originates from rotating the maximum stator current phasor into the fourth quadrant of the complex plane to a limit of under excitation. Finally, the PQ generator capability curve is simply a synchronous generator's (voltage) phasor diagram with a 90° rotation and a *constant* conversion factor of V_ϕ/X_S where V_ϕ is the generator's one-line equivalent terminal voltage and X_S is the synchronous effective 1-line reactance of the generator [108].

In translating the generator capacity constraints to an IV formulation, this work recognizes the practical compromise between 1.) the physical modeling of the underlying complexity of generator characteristics, 2.) the socio-economic design of an *equitable* electricity market that frames all generators within the same set of applicable constraints, and 3.) the mathematical tractability of convex vs non-convex feasible regions. Therefore, it reconfirms Carpentier's box constraints with a constant V_ϕ conversion factor from active and reactive power to generator output current.

$$\mathcal{I}_{RG}^{min} \leq \mathcal{I}_{RG} \leq \mathcal{I}_{RG}^{max} \tag{39}$$

$$\mathcal{I}_{IG}^{max} \leq \mathcal{I}_{IG} \leq \mathcal{I}_{IG}^{max} \tag{40}$$

where $\mathcal{I}_{RG}^{min} = P_G^{min}/V_\phi$, $\mathcal{I}_{RG}^{max} = P_G^{max}/V_\phi$, $\mathcal{I}_{IG}^{min} = Q_G^{min}/V_\phi$, and $\mathcal{I}_{IG}^{max} = P_G^{max}/V_\phi$. Again, because the conversion from a generator's phasor diagram to its capability curve is simply a multiplication by a constant factor, the backward conversion from PQ coordinates in VA units to complex current coordinates is a division by the same factor. An added advantage of Eq. 39 and 40 is that they can be straightforwardly derived from existing ACOPF datasets; be they real or hypothetical test cases.

F. THERMAL LINE FLOW CONSTRAINTS

Next, the thermal line flow constraints in Equation 7 must be expressed in terms of complex voltages and currents.

$$0 \leq \left([A_G \ A_D] \begin{bmatrix} V_{GR} \\ V_{DR} \end{bmatrix}\right) \mathcal{I}_L^* \leq \left([A_G \ A_D] \begin{bmatrix} V_{GR} \\ V_{DR} \end{bmatrix}\right) \overline{\mathcal{I}_L^*} \tag{41}$$

Given the vector of power line impedances Z_L, substituting Ohm's law from Eq. 15 into Equation 41

and simplifying yields:

$$0 \leq \mathcal{I}_{LR}^2 + \mathcal{I}_{LI}^2 \leq |\overline{I_L}|^2 \qquad (42)$$

where $()^2$ is calculated on an element by element basis.

G. VOLTAGE MAGNITUDE CONSTRAINTS

Next, the separable voltage magnitude constraint in Equation 8 is rewritten in rectangular coordinates and then squared

$$\underline{|V_D|}^2 \leq V_{DR}^2 + V_{DI}^2 \leq |\overline{V_D}|^2 \qquad (43)$$

Note that the lower bound on this constraint also introduces a non-convex feasible region; a subject which is given further attention in Section III-J. The generator voltage terminals also have a separable constraint,

$$V_{GR}^2 + V_{GI}^2 \leq |\overline{V_G}|^2 \qquad (44)$$

Note that a lower bound is not required because, the generator voltage magnitude will always be greater than the bus voltage magnitude of the corresponding bus because of the positive flow of generated current.

H. POWER FACTOR CONSTRAINT

The first of two constraints that must be added to the ACOPF formulation is a bounded power factor. While the power factor at each demand-bus is known in the traditional ACOPF, the switch to an IV formulation means that it no longer is. NERC and other grid operators bound the power factor of power injections at a bus to between 0.95 and 1.00 [69], [70].

$$0.95 \cdot \mathbb{1}^{N_D} \leq \frac{P_D}{S_D} \leq \mathbb{1}^{N_D} \qquad (45)$$

where $\mathbb{1}^{N_D}$ is a vector of ones of length N_D, and the division $()/()$ is element-wise. Using the definition of active and complex power, Eq. 45 becomes:

$$0.95 \cdot \mathbb{1}^{N_B} \leq \cos(\theta_{VD} - \theta_{ID}) \leq \mathbb{1}^{N_D} \qquad (46)$$

where again θ_{VD} is the demand bus voltage phase angles and the current withdrawal phase angles $\theta_{ID} = \tan^{-1}(\mathcal{I}_{DI}/\mathcal{I}_{DR})$. Switching from a constraint on $\cos(\theta_{VD} - \theta_{ID})$ to $\tan(\theta_{VD})$ and then converting to rectangular coordinates results in two sets of separable constraints:

$$V_{DI} - V_{DR} \tan(\theta_{VD}^{max}) \leq 0 \qquad (47)$$
$$0 \leq V_{DI} - V_{DR} \tan(\theta_{VD}^{min}) \qquad (48)$$

where $\theta_{VD}^{max} = 18.19° + \theta_{ID}$ and $\theta_{VD}^{min} = -18.19° + \theta_{ID}$. Although the choice of reference bus is entirely arbitrary, the common practice is to choose a bus connected to a generator (via a lead line). In such a case, the reference bus often has among the larger voltage phase angles in the power system. Furthermore, if the reference bus is chosen to have the largest voltage phase angle, then $\theta_{VD}^{max} = 0$.

I. VOLTAGE STABILITY CONSTRAINT

In addition to the above, the power system lines and generator's lead line must maintain voltage stability; expressed as a voltage angle difference inequality constraint.

$$\begin{bmatrix} \Delta\theta_{VG}^{min} \\ \Delta\theta_{VD}^{min} \end{bmatrix} \leq \left(\begin{bmatrix} A_G & A_D \end{bmatrix} \begin{bmatrix} \theta_{VG} \\ \theta_{VD} \end{bmatrix} \right) \leq \begin{bmatrix} \Delta\theta_{VG}^{max} \\ \Delta\theta_{VD}^{max} \end{bmatrix} \qquad (49)$$

where $\Delta\theta_{VD}^{min}$ and $\Delta\theta_{VD}^{max}$ represent vectors of the minimum and maximum voltage phasor angle differences between connected demand buses in the network, and $[\theta_{VG}; \theta_{VD}]$ is the vector of nodal voltage angles.

In most practical applications, $\Delta\theta_{VD}^{min}$, $\Delta\theta_{VD}^{max}$, $\Delta\theta_{VGD}^{min}$, and $\Delta\theta_{VGD}^{max}$ are small in magnitude. Next, Equation 49 can be rewritten as a constraint on the current phase angle using Ohm's law. Given an arbitrary power line l with a voltage difference ΔV_l across it, the current phasor is:

$$\mathcal{I}_l = \frac{|\Delta V_l|e^{i(\Delta\theta_{vl})}}{|z_l|e^{i(\theta_{zl})}} = \frac{|\Delta V_l|}{|z_l|} e^{i(\Delta\theta_{vl} - \theta_{zl})} \qquad \forall l \in \mathcal{L} \qquad (50)$$

Consequently, the vector of current phase angles is:

$$\theta_L = \begin{bmatrix} A_G & A_D \end{bmatrix} \begin{bmatrix} \theta_{VG} \\ \theta_{VD} \end{bmatrix} - \theta_{ZL} \qquad (51)$$

Substituting Eq. 51 into Eq. 49.

$$\theta_L^{min} \leq \theta_L \leq \theta_L^{max} \qquad (52)$$

where $\theta_L^{min} = \Delta\theta_{BV}^{min} - \theta_{ZL}$ and $\theta_L^{max} = \Delta\theta_{VGD}^{max} - \theta_{ZL}$. Equation 52 is then rewritten in rectangular coordinates to yield two sets of separable constraints.

$$I_{LI} - I_{LR} \tan(\theta_L^{max}) \leq 0 \qquad (53)$$
$$0 \leq I_{LI} - I_{LR} \tan(\theta_L^{min}) \qquad (54)$$

where $\tan()$ is calculated on an element by element basis.

J. RELAXING THE NON-CONVEX LOWER BOUND CONSTRAINTS ON VOLTAGE MAGNITUDES

A careful inspection of Equation 43 reveals that the lower bounds on the demand bus voltage magnitudes create a non-convex feasible region. Neglecting the network flow constraints, and taking advantage of the separable nature of the remainder of the IV-ACOPF formulation, a graphical approach serves to develop intuition. Figure 3 shows the feasible region of the real and and imaginary components of the voltage at an arbitrarily chosen demand bus $V_d = V_{Rd} + jV_{Id}$. The "halo"-shaped region in dark grey is caused by the upper and lower bounds on the voltage magnitude in Eq. 43 and corresponds to the original ACOPF problem in Section II. The forrest green region $\mathcal{R}_{FVd}$ is the result of adding the power factor constraints 47 and 48 and corresponds to the new IV-ACOPF formulation. This very intuitive ("crust of a pizza slice") shape, in actuality, is a two-dimensional projection of the multi-dimensional feasible region formed by Eqs. 43, 47, and 48. For simplicity of discussion, the remainder of this paper refers to this multi-dimensional region and its two-dimensional projection interchangeably. Note that the lower

bound constraint makes the feasible region $\mathcal{R}_{FVd}$ non-convex. This is because it is possible to choose two points in the feasible region $\mathcal{R}_{FVd}$ and connect them with a line that leaves the feasible region. From these definitions, it follows that the feasible region of the IV-ACOPF formulation R_F prior to any relaxation is $R_F = \bigcap_{d \in \mathcal{D}} R_{FVd}$.
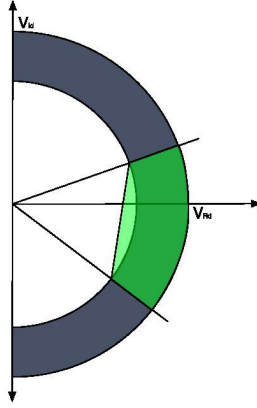

FIGURE 3. Feasible region of the voltage magnitude constraint.

In order to overcome this lack of convexity, this work introduces a high quality relaxation of the feasible region. Graphically, the newly relaxed feasible region $\mathcal{R}_{RF} = \mathcal{R}_F \cup \mathcal{R}_R$ now includes an additional relaxed region $\mathcal{R}_R$ in light green which is formed by the creation of a secant line between the power factor constraints. $\mathcal{R}_R = \bigcap_{d \in \mathcal{D}} \mathcal{R}_{RVd}$.

With respect to the demand bus voltage magnitude lower bounds, they are relaxed to a set of separable secant lines defined by:

$$\left(V_{DR} - \Upsilon_{VDR} \right) = m_{VD} \cdot \left(V_{DI} - \Upsilon_{VDI} \right) \tag{55}$$

where

$$m_{VD} = \frac{\cos(\theta_{VD}^{max}) - \cos(\theta_{VD}^{min})}{\sin(\theta_{VD}^{max}) - \sin(\theta_{VD}^{min})} \tag{56}$$

$$\Upsilon_{VDI} = \underline{|V_D|} \sin(\theta_{VD}^{max}) \tag{57}$$

$$\Upsilon_{VDR} = \underline{|V_D|} \cos(\theta_{VD}^{max}) \tag{58}$$

Note that the secant line is written in the form $V_{DR} = f(V_{DI})$ to avoid the potential for a line with infinite slope.

K. SUMMARY OF IV-ACOPF FORMULATION

The new IV-ACOPF formulation is summarized and recast in the standard form of a convex program.

$$\min \mathcal{J} = \sum_{g \in \mathcal{G}} \left(\alpha_{Zg}(\mathcal{I}_{Rg}^2 + \mathcal{I}_{Ig}^2)^2 + \beta_{Zg}(\mathcal{I}_{Rg}^2 + \mathcal{I}_{Ig}^2) + \gamma_{Rg} + \gamma_{Ig} \right)$$

$$+ \sum_{d \in \mathcal{D}} \left(\bar{\rho}_{Rd}(V_{Rd}I_{Rd} + V_{Id}I_{Id})^2 - \beta_{Rd}(V_{Rd}I_{Rd} \right.$$

$$\left. + V_{Id}I_{Id}) + \bar{\gamma}_{Rd} \right)$$

$$+ \left(\bar{\rho}_{Id}(-V_{Rd}I_{Id} + V_{Id}I_{Rd})^2 - \beta_{Id}(-V_{Rd}I_{Id} \right.$$

$$\left. + V_{Id}I_{Rd}) + \bar{\gamma}_{Id} \right) \tag{59}$$

$$s.t. \quad \begin{bmatrix} \mathcal{I}_{GR} \\ -\mathcal{I}_{DR} \end{bmatrix} - \begin{bmatrix} A_G^T \\ A_D^T \end{bmatrix} \mathcal{I}_{LR} = 0 \tag{60}$$

$$\begin{bmatrix} \mathcal{I}_{GI} \\ -\mathcal{I}_{DI} \end{bmatrix} - \begin{bmatrix} A_G^T \\ A_D^T \end{bmatrix} \mathcal{I}_{LI} = 0 \tag{61}$$

$$\begin{bmatrix} A_G^T \\ A_D^T \end{bmatrix} \mathcal{I}_{LR} - G \begin{bmatrix} V_{GR} \\ V_{DR} \end{bmatrix} + B \begin{bmatrix} V_{GI} \\ V_{DI} \end{bmatrix} = 0 \tag{62}$$

$$\begin{bmatrix} A_G^T \\ A_D^T \end{bmatrix} \mathcal{I}_{LI} - B \begin{bmatrix} V_{GR} \\ V_{DR} \end{bmatrix} - G \begin{bmatrix} V_{GI} \\ V_{DI} \end{bmatrix} = 0 \tag{63}$$

$$V_{I_{ref}} = 0 \tag{64}$$

$$\mathcal{I}_{GR} - \mathcal{I}_{GR}^{max} \leq 0 \tag{65}$$

$$\mathcal{I}_{GR}^{min} - \mathcal{I}_{GR} \leq 0 \tag{66}$$

$$\mathcal{I}_{GI} - \mathcal{I}_{GI}^{max} \leq 0 \tag{67}$$

$$\mathcal{I}_{GI}^{min} - \mathcal{I}_{GI} \leq 0 \tag{68}$$

$$\mathcal{I}_{LR}^2 + \mathcal{I}_{LI}^2 - |\overline{I_L}|^2 \leq 0 \tag{69}$$

$$V_{DR}^2 + V_{DI}^2 - \overline{|V_D|}^2 \leq 0 \tag{70}$$

$$V_{DI} - V_{DR}\tan(\theta_{VD}^{max}) \leq 0 \tag{71}$$

$$V_{DR}\tan(\theta_{VD}^{min}) - V_{DI} \leq 0 \tag{72}$$

$$V_{GR}^2 + V_{GI}^2 - \overline{|V_G|}^2 \leq 0 \tag{73}$$

$$\mathcal{I}_{LI} - \mathcal{I}_{LR}\tan(\theta_L^{max}) \leq 0 \tag{74}$$

$$\mathcal{I}_{LR}\tan(\theta_L^{min}) - \mathcal{I}_{LI} \leq 0 \tag{75}$$

$$\left(V_{DR} - \Upsilon_{VDR} \right) - m_{VD}\left(V_{DI} - \Upsilon_{VDI} \right) \leq 0 \tag{76}$$

where the convex constraint in Eq. 76 is the relaxation the non-convex constraint

$$-V_{DR}^2 - V_{DI}^2 + \underline{|V_D|}^2 \leq 0 \tag{77}$$

It is worth emphasizing that the objective function is separable with respect to each of the generators and demand buses.

$$\mathcal{J} = \sum_{g \in \mathcal{G}} \mathcal{J}_g(\mathcal{I}_{Rg}, \mathcal{I}_{Ig}) + \sum_{d \in \mathcal{D}} \mathcal{J}_d(V_{Rd}, V_{Id}) \tag{78}$$

Meanwhile, with the exception of the network flow constraints in Eq. 60-63, all of the constraints are separable with respect to generators and demand buses as well.

L. CONVEXITY ANALYSIS OF THE FINAL FORMULATION

In order to develop a solution algorithm in the following section, a convexity proof is provided.

Theorem 1: The optimization program described by the objective function 59 and subject to constraints 60-76 is a convex optimization program.

Proof: The objective function as expressed in Eq. 59 is a sum of separable functions of the generator current variables and the demand bus voltage variables. Therefore, the convexity of each of these can be determined independently. The generator cost terms take the form $\sum_g f_g(h_g(\mathcal{I}_{Rg}, \mathcal{I}_{Ig}))$. $h_g()$ is stated in terms of two variables and has a Hessian